Available online at www.sciencedirect.com

ScienceDirect

Biochimica et Biophysica Acta 1768 (2007) 2280–2292

Biochimica et Biophysica Acta BBA

www.elsevier.com/locate/bbamem

Transfection efficiency boost by designer multicomponent lipoplexes

Giulio Caracciolo [a], Daniela Pozzi [a], Ruggero Caminiti [a,*], Cristina Marchini [b], Maura Montani [b], Augusto Amici [b], Heinz Amenitsch [c]

[a] Department of Chemistry, University of Rome "La Sapienza", P.le A. Moro 5, 00185 Rome, Italy

[b] Genetic Immunization Laboratory, Department of Molecular Cellular and Animal Biology, University of Camerino, Via Camerini 5, 62032 Camerino (MC), Italy

[c] Institute of Biophysics and Nanosystems Research, Austrian Academy of Sciences, Schmiedelstrasse 6, A-8042 Graz, Austria

Received 26 January 2007; received in revised form 25 June 2007; accepted 27 June 2007
Available online 6 July 2007

Abstract

Cationic liposome–DNA complexes (lipoplexes) have emerged as leading nonviral gene carriers in worldwide gene therapy clinical trials. Arriving at therapeutic dosages requires the full understanding of the mechanism of transfection. We investigated the correlation between structural evolution of multicomponent lipoplexes when interacting with cellular lipids, the extent of DNA release and the efficiency in transfecting mouse fibroblast (NIH 3T3), ovarian (CHO) and tumoral myofibroblast-like (A17) cell lines. We show, for the first time, that the transfection pattern increases monotonically with the number of lipid components and further demonstrate by means of synchrotron small angle X- ray scattering (SAXS) that structural changes of lipoplexes induced by cellular lipids correlate with the transfection efficiency. Specifically, inefficient lipoplexes either fused too rapidly upon interaction with anionic lipids or, alternatively, are found to be extremely resistant to solubilization. The most efficient lipoplex formulations exhibited an intermediate behaviour. The extent of DNA unbinding (measured by electrophoresis on agarose gel) correlates with structural evolution of the lipoplexes but DNA-release does not scale with the extent of transfection. The general meaning of our results is of broad interest in the field of non-viral gene delivery: rational adjusting of lipoplex composition to generate the proper interaction between lipoplexes and cellular lipids may be the most appropriate strategy in optimizing synthetic lipid transfection agents.

Keywords: Cationic liposome; DNA; Lipoplex; Gene delivery; Transfection efficiency; SAXS

1. Introduction

Synthetic cationic liposomes (CLs) form stable complexes with polyanionic DNA [1]. CL–DNA complexes, named lipoplexes, have recently emerged as leading nonviral vectors in worldwide gene therapy clinical trials. Unfortunately, their present low transfection activity severely compromises their systematic use both *in vitro* and *in vivo*. Improving transfection efficiency (TE) of lipoplexes requires answers to some specific questions: what is the mechanism of formation of lipoplexes, what is the correlation between the physical attributes of lipoplexes and their functional activity? Usually, lipoplexes are organized in multilamellar structures (L_α^C phase) with DNA embedded with cationic lipid membranes [2–4]. Less frequently, an inverted hexagonal H_{II}^C phase comprised of lipid-coated DNA strands arranged on a hexagonal lattice has been observed [4]. Even though some earlier studies suggested superiority in transfection of hexagonal lipoplexes with respect to lamellar ones [4], experimental evidence negated a correlation between structure and activity [5–7]. However, recent experiments have disputed this suggestion [7,8], but there is general consensus that a direct correlation between initial lipoplexes structure and transfection efficiency does not exist [7,9].

Unfortunately, the mechanism of interaction of lipoplexes with cell membranes remains poorly understood. As a result, the structural evolution of lipoplexes upon interaction and mixing with cellular lipids has been attracting a great number of scientists in the field of non-viral gene delivery. Hereby the structural changes of lipid carriers resulting in DNA release may be the key step in lipid-mediated DNA delivery (lipofection) [9–13]. At the same time, more efficient synthetic reagents are highly desirable.

* Corresponding author. Tel.: +39 06 4991 3661; fax: +39 06 490631.
E-mail address: r.caminiti@caspur.it (R. Caminiti).

0005-2736/$ - see front matter © 2007 Elsevier B.V. All rights reserved.
doi:10.1016/j.bbamem.2007.06.027

To this end, we prepared multicomponent lipoplexes incorporating from three to six lipid components within the lipid bilayer [14,15]. Recently, we have demonstrated the superiority in transfection of multicomponent lipoplexes with respect to binary ones usually employed for gene delivery [16]. For instance, the four-component lipid system incorporating cationic lipids 1,2-dioleoyl-3-trimethylammonium-propane (DOTAP) and (3β-[*N*-(*N*′,*N*′-dimethylaminoethane)-carbamoyl])-cholesterol (DC-Chol) and neutral helper lipids dioleoylphosphocholine (DOPC) and dioleoylphosphatidylethanolamine (DOPE) transfected DNA into mouse fibroblast (NIH 3T3) and tumoral myofibroblast-like (A17) cell lines more efficiently than DOTAP−DOPC and DC-Chol−DOPE cationic liposomes separately.

It is currently accepted, and several evidences exist, that lipoplexes are internalized into the cytoplasm by endocytosis and that fuse with the negatively charged cellular membranes [6]. It is a central point since fusogenicity is considered to contribute significantly to cytoplasmic delivery of DNA [17]. Many investigators have shown that lipid mixtures are more fusogenic than single lipids. Such a phenomenon has been related to nonideal mixing of lipid components [18,19], formation of lipid rafts [19] (that may play a role in membrane recognition) and higher probability for packing defects in mixtures relative to single component bilayers [18]. Furthermore, preparation of liposomes incorporating very different lipid headgroups and/or aliphatic chains has been shown to produce asymmetric vesicles [20]. Such an asymmetry is expected to increase the biocompatibility and flexibility of vesicle drug delivery systems [20]. According to all these suggestions, multicomponent lipoplexes may be more fusogenic, biocompatible and flexible gene carriers than binary lipoplexes.

Thus, we have extended our previous study to investigate how transfection changes with increasing number of lipid components the synthetic carrier is made of. With the aim of providing new insights into the mechanism of transfection, we also investigated the structural evolution of lipoplexes upon interaction with cellular (anionic) lipids by means of synchrotron small angle X-ray scattering (SAXS). First, the existence of different regimes of stability was demonstrated: inefficient complexes were either easily disintegrated by anionic lipids (regime of instability) or definitely too resistant (regime of high stability). The most efficient lipoplexes exhibited intermediate 'optimal stability'. Secondly, to correlate structural changes of lipoplexes and DNA release, we also measured the extent of DNA release by electrophoresis after addition of negatively charged lipids to preformed lipoplexes. The extent of DNA unbinding correlates strictly with the instability of lipoplexes, but we note that the DNA release is not proportional to the transfection efficiency. On the basis of our results, here we advance the concept that the structural stability of lipoplexes against anionic lipids is the critical factor regulating transfection efficiency by lipoplexes.

2. Materials and methods

2.1. Cationic liposomes preparation

Cationic 1,2-dioleoyl-3-trimethylammonium-propane (DOTAP) and (3β-[*N*-(*N*′,*N*′-dimethylaminoethane)-carbamoyl])-cholesterol (DC-Chol), anionic dioleoylphosphatidylglycerol (DOPG) and neutral dioleoylphosphatidylethanolamine (DOPE), dioleoylphosphocholine (DOPC), 1,2-dilauroyl-*sn*-glycero-3-phosphocholine (DLPC) and 1,2-dimyristoyl-*sn*-glycero-3-phosphocholine (DMPC) were purchased from Avanti Polar Lipids (Alabaster, AL) and used without further purification. DOTAP–DOPC, DOTAP–DLPC, DOTAP–DOPE, DC-Chol–DOPE and DC-Chol–DMPC cationic liposomes were prepared according to standard protocols [21]. In brief, each binary mixture, at a molar fraction of neutral lipid in the bilayer X_N=(neutral lipid/total lipid) (mol/mol)=0.5, was dissolved in chloroform and the solvent was evaporated under vacuum for at least 24 h. The obtained lipid films were hydrated with the appropriate amount of Tris–HCl buffer solution (10^{-2} M, pH 7.4) to achieve the desired final concentration (10 mg/ml for the X-ray samples). The obtained liposome solutions were stored at 30 °C for 24 h to achieve full hydration. Indeed, we have recently found evidence that lipid hydration is important to achieve the equilibrium structure of lipoplexes [22]. The same protocol was followed to prepare anionic liposomes (AL) made of DOPG. Negatively charged liposomes mimicking membrane lipid composition were also prepared (MM=DOPC:DOPE:DOPG, 1:1:1 molar ratio).

2.2. Lipoplexes preparation

Calf thymus Na-DNA was purchased from Sigma-Aldrich (St. Louis, MO). DNA was dissolved in Tris–HCl buffer (5 mg/ml) and was sonicated for 5 min inducing a DNA fragmentation with length distribution between 500 and 1000 base pairs, which was determined by gel electrophoresis. Plasmid DNA (pGL3 which codifies for firefly luciferase) was purchased from Promega (Madison, WI). By mixing adequate amounts of the DNA solutions to suitable volumes of liposome dispersions, self-assembled DOTAP–DOPC/DNA, DOTAP–DLPC/DNA, DOTAP–DOPE/DNA, DC-Chol–DOPE/DNA and DC-Chol–DMPC/DNA binary lipoplexes were obtained. To examine the effect of DNA kind (linear or plasmid) on the structure of lipoplexes, both CL-linear DNA and CL-plasmid DNA complexes were prepared. Multicomponent lipoplexes were prepared by adding DNA to mixed lipid dispersions made of distinct populations of CLs. For instance, DOTAP–DOPC (1:1) plus DOTAP–DLPC (1:1) loaded with DNA results in DOTAP–DOPC–DLPC/DNA complexes (2:1:1). In such a manner, multicomponent lipoplexes, incorporating from three to six lipid species, were formed in a self-assembled manner [14,15]. Further all samples were prepared with the same cationic lipid/DNA ratio (mol/mol), i.e. ρ=(cationic lipid (by mole)/DNA base)=3.2. The chosen charge ratio (positively charged lipoplexes) guarantees maximum DNA load, which is not the case for isoelectric complexes (ρ=1). In Table 1 the lipoplexes are listed as a function of increasing membrane charge density that was calculated according to ref. [6].

After storage for 3 days at 4 °C, allowing the samples to reach equilibrium, they were transferred to 1.5 mm diameter quartz X-ray capillaries (Hilgenberg, Malsfeld, Germany). The capillaries were centrifuged for 5 min at 6000 rpm at room temperature to consolidate the samples.

Table 1
Cationic liposomes listed as a function of increasing membrane charge density, σ_M

Lipid composition	σ_M 10^{-3} (e/Å^2)
DOTAP–DOPC (1:1)	7.6
DOTAP–DOPC–DLPC (2:1:1)	7.6
DOTAP–DLPC (1:1)	7.9
DOTAP–DC-Chol–DOPC (1:4:5)	8.1
DOTAP–DC-Chol–DOPC (5:2:3)	8.2
DOTAP–DC-Chol–DMPC–DLPC (1:1:1:1)	8.4
DOTAP–DC-Chol–DOPC–DOPE–DMPC–DLPC (2:2:1:1:1:1)	8.5
DOTAP–DC-Chol–DOPC–DOPE (1:1:1:1)	8.5
DOTAP–DC-Chol–DMPC–DLPC (1:1:1:1)	8.7
DOTAP–DC-Chol–DOPE–DLPC (1:1:1:1)	8.9
DOTAP–DC-Chol–DOPE–DMPC (1:1:1:1)	9.4
DC-Chol–DMPC (1:1)	9.4
DC-Chol–DOPE–DMPC (1:1)	9.6
DC-Chol–DOPE (1:1)	9.8

2.3. Lipoplexes/anionic liposomes systems preparation

Lipoplexes and anionic liposomes made of DOPG or MM liposomes were mixed at different anionic/cationic charge ratios $R=0$, 0.1, 0.2, 0.5, 1, 2, 3, 4, 5, 7, 8, 9, 10, 15, 20, 25. These mixed dispersions were then equilibrated for 2 days, filled into quartz capillaries, and flame-sealed. Final concentration of samples was 10 mg/ml. To ensure equilibration the samples were kept at 4 °C for 2 days. As kinetic experiments demonstrated (see section 3.4. Kinetics of structural changes of lipoplexes induced by anionic lipids and section 3.7. Kinetics of DNA release from lipoplexes induced by anionic lipids), to reach equilibrium 2 days are more than sufficient.

2.4. Transfection efficiency experiments

Cell lines were cultured in Dulbecco's modified Eagle's medium (DMEM) (Invitrogen, Carlsbad, CA) supplemented with 1% penicillin–streptomycin (Invitrogen) and 10% fetal bovine serum (FBS, Invitrogen) at 37 °C and 5% CO_2 atmosphere, splitting the cells every 2–4 days to maintain monolayer coverage. For luminescence analysis, mouse fibroblast NIH 3T3, ovarian CHO and tumoral myofibroblast-like A17 cells were transfected with pGL3 control plasmid (Promega). The day before transfection, cells were seeded in 24 well plates (150000 cells/well) using medium without antibiotics. Cells were incubated until they were 75–80% confluent, which generally took 18 to 24 h. For TE experiments, lipoplexes were prepared in Optimem (Invitrogen) by mixing for each well of 24 well plates 0.5 μg of plasmid with 5 μl of sonicated lipid dispersions (1 mg/ml). These complexes were left for 20 min at room temperature before adding them to the cells. The cells were incubated with lipoplexes in Optimem (Invitrogen) for 6 h to permit transient transfection; the medium was then replaced with DMEM supplemented with FBS. Luciferase expression was analyzed after 48 h and measured with the Luciferase Assay System from Promega, and light output readings were performed on a Berthold AutoLumat luminometer LB-953 (Berthold, Bad Wildbad, Germany). TE was normalized to milligrams of total cellular protein in the lysates using the Bio-Rad Protein Assay Dye Reagent (Bio-Rad, Hercules, CA).

2.5. Synchrotron small angle X-ray scattering measurements

All X-ray measurements were performed at the Austrian SAXS station of the synchrotron light source ELETTRA (Trieste, Italy) [23]. SWAXS patterns were recorded with two gas detectors based on the delay line principle covering q-ranges ($q=4\pi sin(\theta)/\lambda$) of between 0.05 and 0.6 $Å^{-1}$ (SAXS regime) and between 1.2 and 1.8 $Å^{-1}$ (WAXS regime). The angular calibration of the detectors was performed with silver-behenate powder (d-spacing=58.38 Å) for the SAXS regime and with p-bromobenzoic acid for the WAXS regime. The data have been normalized for variations of the primary beam intensity, corrected for the detector efficiency and the background has been subtracted. The temperature was controlled in the vicinity of the capillary to within±0.1 °C (Anton Paar, Graz, Austria). Exposure times were typically 300 s. No evidence of radiation damage was observed in the X-ray diffraction patterns.

2.6. Small angle X-ray scattering data analysis

Bragg peak positions, widths and intensities of some diffraction patterns were analyzed by multiple fitting of Lorentzian distributions [2]. Further, in the case of DOPG the bilayer thickness, d_B (head to head group distance), was calculated by standard procedures, i.e. the electron density profile was deduced from the diffraction data. For further details see the protocols given in [24–27].

2.7. Agarose gel electrophoresis experiments

Electrophoresis studies were conducted on 1% agarose gels containing Tris-Borate-EDTA (TBE) buffer. After electrophoresis ethidium bromide (Et-Br) was added and then visualized. Lipoplexes were prepared by mixing 40 μl of lipid dispersions (1 mg/ml, Tris–HCl buffer) with 4 μg of pGL3 control plasmid. These complexes were let to equilibrate for 3 days at 4 °C before adding negatively charged liposomes (DOPG or MM). After 24 h, naked plasmid DNA, lipoplexes and lipoplexes/AL systems with different R were analyzed by electrophoresis. For this purpose, 20 μl of each sample was mixed with 4 μl of loading buffer (glycerol 30% v/v, bromophenol blue 0.25% v/v) and subjected to agarose gel electrophoresis for 1 h at 80 V. The electrophoresis gel was visualized and digitally photographed using a Kodak Image Station, model 2000 R (Kodak, Rochester, NY). Digital photographs were elaborated using a dedicated software (Kodak MI, Kodak) that allows to calculate the molar fraction of released DNA, X_{DNA}.

2.8. Dynamic light scattering experiments

Size of liposomes and lipoplexes were measured at the temperature of 25 °C by means of dynamic light scattering (DLS) technique, using a Malvern Zetasizer4 apparatus (Malvern Instruments, Malvern, UK). The normalized intensity autocorrelation functions detected at 90° angle were analyzed by using the CONTIN procedure [28]. For all the samples investigated, data show a unimodal distribution and represent the average of at least four different measurements carried out for each sample. The apparent hydrodynamic radius, R_H, was calculated according to ref. [28].

3. Results

3.1. Transfection efficiency results

In our previous study [16] we showed that four-component lipoplexes exhibited higher transfection efficiency than binary ones usually employed for gene delivery purposes. To extend that research, we asked ourselves whether the transfection curve changes proportional with the number of lipid components, n, the lipid system is composed of. To address this issue, we prepared several lipoplexes varying composition of lipid bilayer and observed how transfection varied. We performed transient transfection assay of mouse fibroblast NIH 3T3, ovarian CHO and tumoral myofibroblast-like A17 cell lines. It is well known that transfection efficiency is strongly influenced by the relative proportions of cationic lipid, colipid, and DNA [29,30]. Specifically, the neutral lipid/total lipid molar ratio, X_N, influences the structure and thermotropic phase behaviour of lipoplexes [22,26,27,31]. This can affect the plasmid uptake, opsonization, and endosomal entrapment [32]. The charge ratio is another critical parameter. Minimizing the amount of cationic lipid is desirable to reduce potential toxic effects, while high cationic lipid content is needed to complex with and neutralize the large number of negative charges of DNA. To accomplish both these requirements, all the CLs were formed with equimolar fraction of cationic and neutral lipid ($X_C=X_N=0.5$) and were prepared with the same charge ratio $\rho=3.2$. To prove the effect of charge ratio of lipoplexes on TE, we performed preliminary measurements on the three cells lines at three distinct charge ratios: 2.4, 2.8 (both not reported) and 3.2. When plotted against the charge ratio, TE essentially remained almost constant for each lipid formulation. Our results were in very good agreement with the recent results provided by the Safinya's group [33,34], who investigated in great detail the role of ρ on TE. Thus, the chosen $\rho=3.2$ in our performed SAXS and electrophoresis measurements are justified.

Fig. 1 shows transfection efficiency data for the tested lipoplex formulations in three cell lines, namely, NIH 3T3 (bottom panel), CHO (middle panel) and A17 (top panel) cell lines. For clarity, histograms with the same abscissa in different

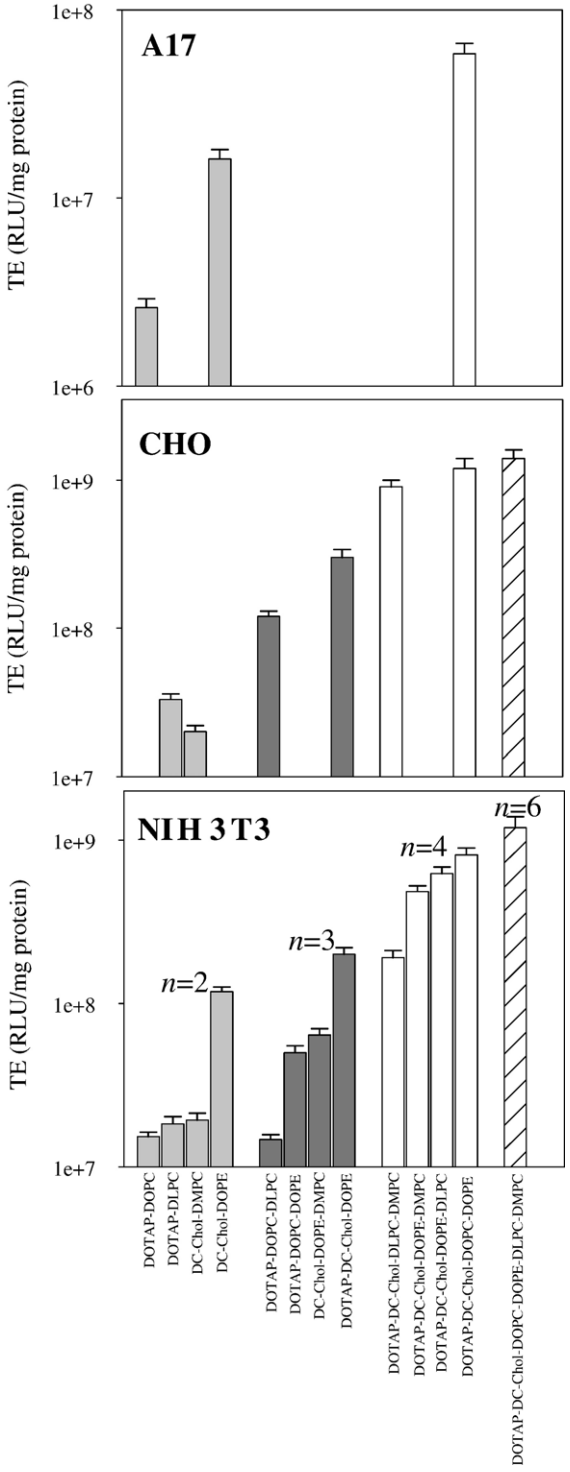

Fig. 1. Transfection efficiency data for the tested lipoplex formulations in three cell lines: NIH 3T3 (bottom panel), CHO (middle panel) and A17 (top panel). For clarity, histograms with the same abscissa in different panels refer to the same lipid formulation. Each colour refers to lipoplex formulations with the same number of lipid components, namely, $n=2$ (gray), 3 (dark gray), 4 (white) and 6 (coarse pattern). Multicomponent lipoplexes ($n=4$, 6) presented much higher TE (about two orders of magnitude) than binary lipoplexes usually employed for gene delivery.

panels refer to the same lipoplex formulation and each colour refers to lipoplex formulations with the same number of lipid components. All formulations tested display a transfection activity which monotonically increases with the number of lipid components, n. In the case of NIH 3T3 cells, TE reached a maximum (TE $\sim 2\times10^9$ RLU/mg) at the highest $n=6$. Even though the overall effect is quite clear, we observed that not only the number of lipid components, but also lipid composition altered transfection activity significantly. For example, DOTAP–DOPC/DNA ($X_{DOTAP}=0.5$, $X_{DOPC}=0.5$) lipoplexes were found to be equally efficient, within experimental errors, to those of the three-component DOTAP–DOPC–DLPC/DNA ($X_{DOTAP}=0.5$, $X_{DOPC}=0.25$, $X_{DLPC}=0.25$) systems. This indicates that the use of two colipids (DOPC and DLPC) instead of a single one (DOPC) does not always give higher TE. For $n=3$, DOTAP–DOPC–DOPE/DNA ($X_{DOTAP}=0.5$, $X_{DOPC}=0.25$, $X_{DOPE}=0.25$) systems were 2-fold more efficient than DOTAP–DOPC–DLPC/DNA ($X_{DOTAP}=0.5$, $X_{DOPC}=0.25$, $X_{DLPC}=0.25$) complexes. Thus, at a fix number of lipid components, DOPE as a colipid

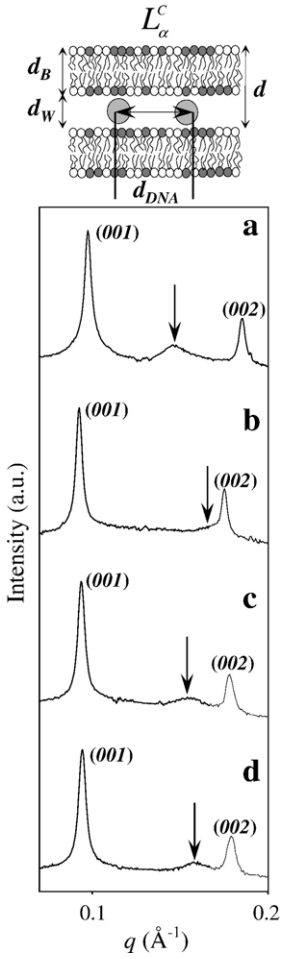

Fig. 2. Representative SAXS patterns of lipoplexes as a function of increasing number of lipid components: DOTAP–DOPC/DNA (a), DC-Chol–DOPE–DMPC/DNA (b), DOTAP–DC-Chol–DOPC–DOPE/DNA (c) and DOTAP–DC-Chol–DOPC–DOPE–DLPC–DMPC/DNA (d). Interhelical DNA–DNA distance peak is marked by an arrow and shifts as a function of lipid composition. As the membrane charge density increases (from top to bottom) the DNA load augments accordingly. On the top, schematics of the inner structure of lamellar CL–DNA complexes is shown. In the lamellar phase, L_α^C, composed of alternative lipid bilayers and DNA/water layers, the repeat spacing is given by $d=d_W+d_B$.

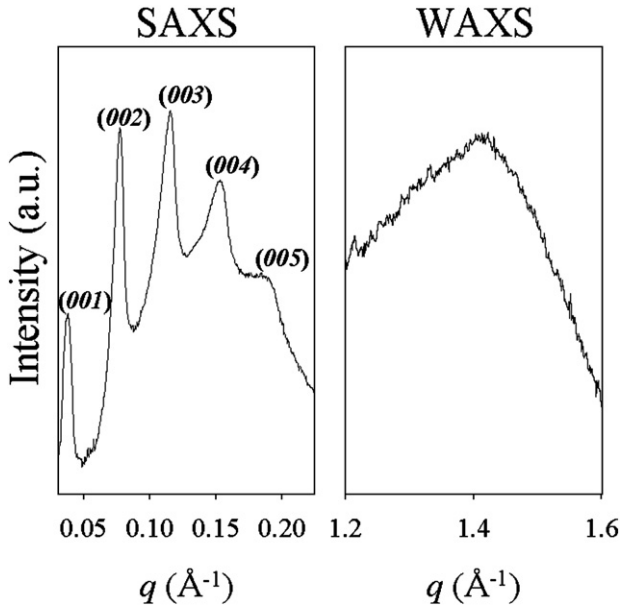

Fig. 3. SAXS pattern of DOPG (left panel). Lamellar Bragg reflections (*00l*) are indicated. The corresponding diffuse WAXS peak around 1.4 $Å^{-1}$ (right panel) displays the in-plane order of the hydrocarbon chains and demonstrates that DOPG membranes are assembled in the fluid phase.

gave higher transfection in DOTAP-containing lipoplexes. The same effect was observed in the case of DC-Chol-containing lipoplexes. Indeed, TE of DC-Chol−DOPE/DNA ($X_{\text{DC-Chol}}=0.5$, $X_{\text{DOPE}}=0.5$) lipoplexes was about 2-fold higher than that of DC-Chol−DOPE−DMPC/DNA ($X_{\text{DC-Chol}}=0.5$, $X_{\text{DOPE}}=0.25$, $X_{\text{DMPC}}=0.25$). This makes DOPE a popular choice as a colipid, and explains why complexes with DOPE are abundant in the literature [30,35]. Our transfection studies showed that also cationic lipids can alter activity of lipoplexes. For instance, DOTAP−DC-Chol−DOPE/DNA lipoplexes ($X_{\text{DOTAP}}=0.25$, $X_{\text{DOPC}}=0.25$, $X_{\text{DOPE}}=0.5$) were about 3-fold more efficient than DC-Chol−DOPE/DNA ones. It means that transfection activity varied significantly with a minor change in cationic lipid composition. Similar trends were also observed for $n=4$ and 6. Last, as Fig. 1 clearly shows, CHO and A17 cell lines show similar results as NIH 3T3.

3.2. Structure of lipoplexes

Synchrotron SAXS experiments revealed the nanostructure of lipoplexes. All lipoplexes were arranged into lamellar arrays, (lamellar L_{α}^{C} phase, Fig. 2). Fig. 2 shows typical SAXS patterns of multicomponent lipoplexes with increasing number of lipid components ($n=2$ (a); $n=3$ (b); $n=4$ (c); $n=6$ (d)). The sharp peaks labelled at q_{00l} arise from the electron density contrast normal to the lipid bilayer. The repeat distance, d, can be decomposed in the membrane thickness (d_B) and the thickness of the water/DNA layer (d_W): $d=d_B+d_W=2\pi/q_{001}$ (Fig. 2). The low-intensity diffuse peak present in the SAXS patterns (marked by arrows) is due to the 1-dimensional DNA interhelical spacing $d_{\text{DNA}}=2\pi/q_{\text{DNA}}$ (Fig. 2). Fig. 2 also illustrates that the 'DNA peak' position changes as a function of lipid composition of lipoplexes, i.e. as a function of the number and kind of lipid molecules assembling the bilayer. Since surface charge density of lipid membranes, σ_M, is the only physical constraint regulating DNA packing density within lipid/DNA complexes [36–38] it means that adjusting lipid composition of multicomponent lipoplexes allows to regulate cationic membranes with specific membrane charge densities (Table 1). Each SAXS pattern arose from a single lamellar phase with a specific DNA load (i.e. a single DNA peak appeared on each diffraction

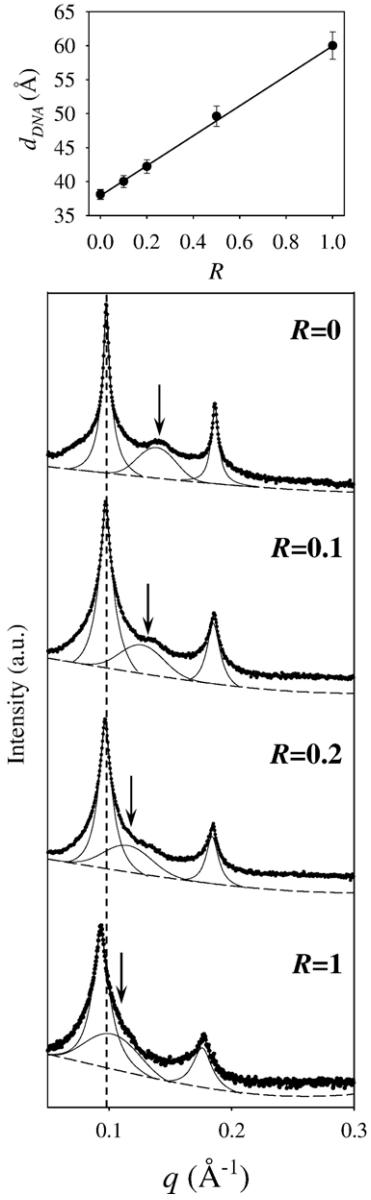

Fig. 4. SAXS patterns of DOTAP−DLPC/DNA lipoplexes as a function of increasing anionic/cationic charge ratio, R (from the top to the bottom). The interhelical DNA–DNA peak shifted to lower q-values as a function of increasing R. This indicates that DNA is progressively diluted by anionic lipids. Vertical dashed line identifies the position of the (001) Bragg peak at $R=0$. Anionic lipids induce a swelling (shift of the diffraction peaks) and enhanced local disorder (broadening of diffraction peaks) of the lamellar phase of lipoplexes. Solid lines indicate the fitting functions while dashed lines represent the non-linear background. The top panel shows the DNA interdistance, d_{DNA}, as a function of R. Solid line is the best linear fit to the data.

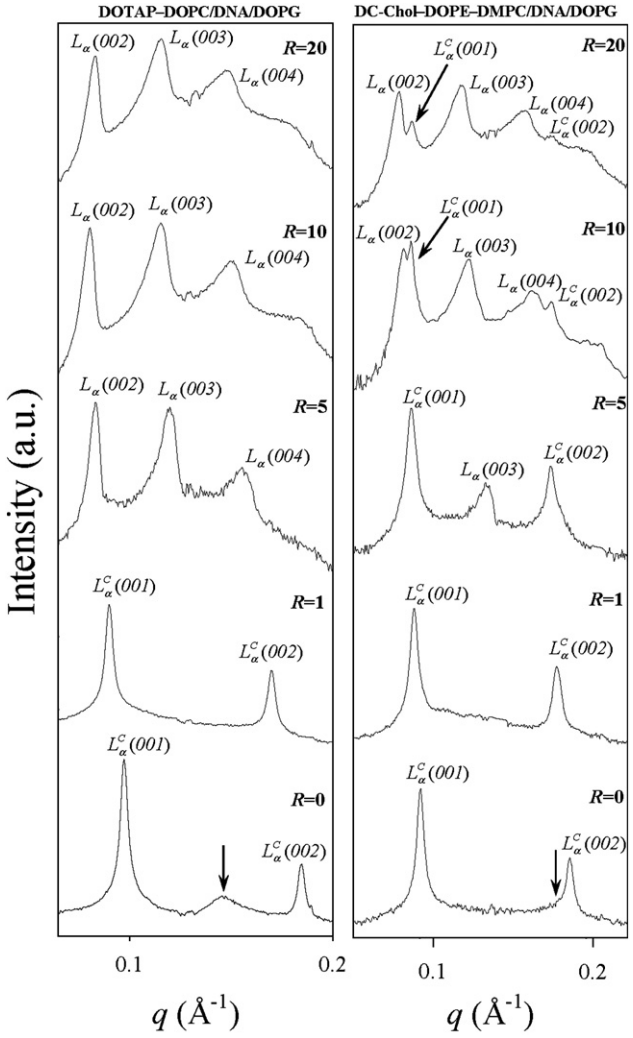

Fig. 5. SAXS patterns of DOTAP–DOPC/DNA (left panel) and DC-Chol–DOPE–DMPC/DNA (right panel) lipoplexes as a function of increasing anionic/cationic charge ratio, *R*.

pattern). This finding confirmed that lipid components were ideally mixed within the membrane of lipid carriers [39].

The SAXS pattern of pure DOPG (Fig. 3, left panel) showed 5 diffraction peaks indexed as the (*00l*) reflections arising from a lamellar phase with repeat distance $d=131.2$ Å. The in-plane packing of the hydrocarbon chains was evaluated by WAXS experiments (Fig. 3, right panel). The WAXS peak ($1.2<q<1.6$ Å^{-1}) with a corresponding *d*-value of about 4.5 Å provides evidence that the system is in the fluid state. From the electron density profile (not reported), both the thickness of the DOPG bilayer ($d_B=34.1$ Å) and that of the interbilayer water region ($d_W=97.1$ Å) were derived. These values were in agreement with those previously obtained for negatively charged POPG liposomes [40].

3.3. Structural changes of lipoplexes induced by anionic lipids

Next, we were particularly interested in whether the structural changes of lipoplexes might correlate with the TE data reported above. To this end, we investigated the structural evolution of lipoplexes when interacting with anionic dioleoylphosphatidylglycerol (DOPG) and MM liposomes as a function of the anionic/cationic charge ratio, *R*, using synchrotron SAXS. DOPG is an anionic lipid common in mammalian cells, in particular in lysosomal membranes and mitochondrial inner membranes. First, for $0<R<1$, the SAXS pattern showed that the 'DNA peak' shifted to lower *q*-values as a function of increasing *R*. For instance, in the case of DOTAP–DLPC/DNA lipoplexes, the interhelical distance, d_{DNA}, changed from 38.1 Å at $R=0$ up to more than 60 Å at $R=1$ (Fig. 4, top panel). This finding indicates that the DNA load was diluted by increasing share of anionic lipids, but the lamellar structure of lipoplexes was not perturbed. Second, for an extended range of *R*-values the phase behaviour of the tested lipoplexes/DOPG mixtures is summarized in Fig. 5 (left panel) showing the SAXS patterns of the DOTAP–DOPC/DNA/DOPG system. At $R=1$, the lamellar phase of lipid/DNA complex is still preserved while, at $R=5$, disintegration of lipoplexes was complete. Fig. 5 (right panel) shows the SAXS patterns of DC-Chol–

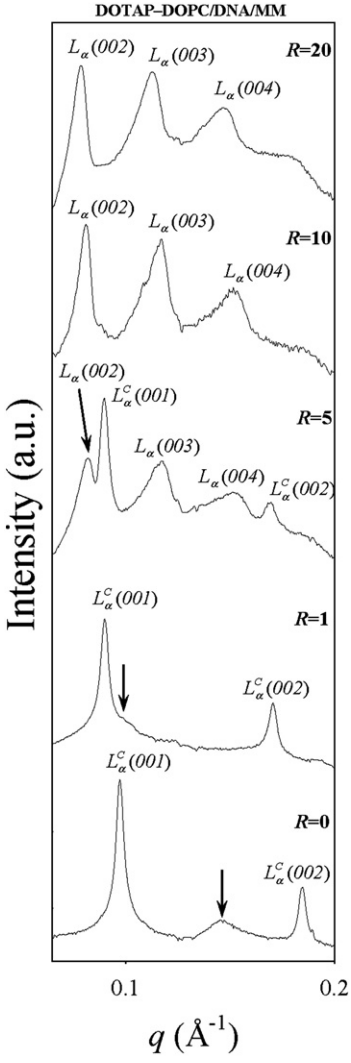

Fig. 6. SAXS pattern of DOTAP–DOPC/DNA/MM mixed systems as a function of increasing anionic/cationic charge ratio, *R*.

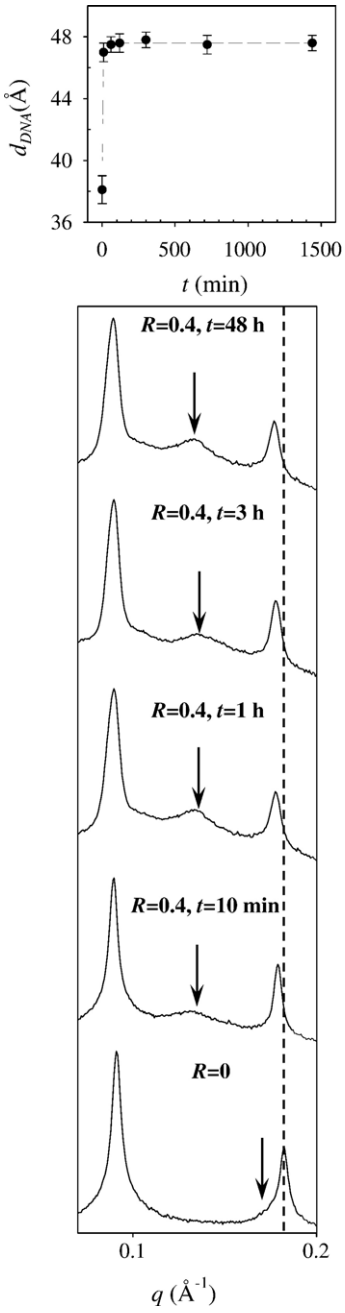

Fig. 7. SAXS patterns of DC-Chol–DOPE /DNA lipoplexes in the time interval from 10 min to 48 h after the addition of negatively charged MM liposomes (R=0.4) compared to that of DC-Chol–DOPE/DNA lipoplexes with no anionic lipid added (R=0). In the top panel the change in interhelical DNA distance with time is shown. The dashed line is the best exponential fit to the data.

DOPE–DMPC/DNA/DOPG complexes as a function of increasing R. As evident, these lipoplexes were much more resistant than DOTAP–DOPC/DNA complexes. Indeed, at R=20, the lamellar DC-Chol–DOPE–DMPC/DNA complexes still resisted disintegration by DOPG as shown by the presence of the (001) (indicated by an arrow) and (*002*) Bragg reflections. For better comparison of the data, we define R* as the anionic/cationic charge ratio at which lipid bilayer disintegration is completed. R* is found to be strongly dependent on the lipoplex formulation. Our findings indicate the existence of a strict correlation between lipoplex formulations and their propensity to be disintegrated by anionic lipids. Specifically, some formulations, such as DOTAP–DOPC, were easily destroyed by anionic lipids, while other formulations, such as DC-Chol–DOPE–DMPC, were definitely more resistant to be disintegrated by anionic lipids.

Figs. 5 (left panel) and 6 together show the comparison between the SAXS patterns of DOTAP–DOPC/DNA/DOPG and DOTAP–DOPC/DNA/MM systems at increasing R values. Lipoplexes/MM mixed systems retained their lamellar structure for longer than did lipoplexes/DOPG mixed systems. For example, at R=1, the DNA peak was not detected on the SAXS pattern of DOTAP–DOPC/DNA/DOPG lipoplexes (probably it was hidden by the (001) Bragg reflection of the lamellar phase of lipoplexes), whereas it was still present on that of DOTAP–DOPC/DNA/MM ones (indicated by an arrow). At R=5, DOTAP–DOPC/DNA lipoplexes were completely disintegrated by DOPG liposomes as shown by the vanishing of the L_{α}^{C} (*00l*) Bragg peaks while they partly resisted disintegration when mixed with MM liposomes.

As a general rule, disintegration of lipoplexes by MM liposomes occurred at higher R* values than those needed when using pure DOPG liposomes. Analogous results (not reported) were obtained with all other lipoplex formulations tested.

3.4. Kinetics of structural changes of lipoplexes induced by anionic lipids

Synchrotron SAXS experiments were also performed to investigated the kinetic structural changes of lipoplexes after addition of anionic lipids. These experiments were necessary to guarantee that structural changes of lipoplexes/anionic liposomes systems equilibrated for 1–2 days were comparable with TE data, which face reaction times of hours, but not for days.

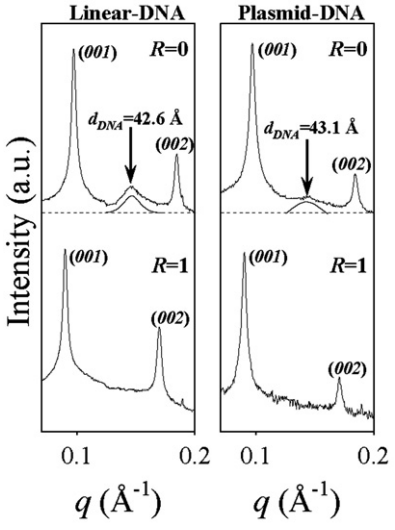

Fig. 8. SAXS patterns of DOTAP–DOPC/linear DNA (left panel) and DOTAP–DOPC/plasmid DNA (right panel) lipoplexes in the absence of anionic lipid (R=0) and with anionic lipid added (R=1). Solid lines represent the best fits to the 'DNA peak'.

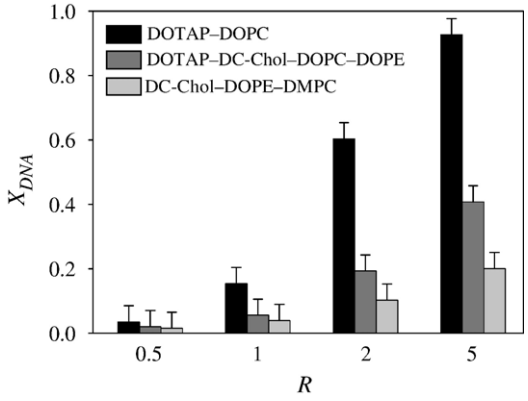

Fig. 9. Effect of lipid composition on the DNA release capacity of lipoplexes investigated by electrophoresis on agarose gels as a function of increasing *R*. As evident, X_{DNA} raised with increasing *R*. At each *R* value, the molar fraction of released DNA was in the following order: DOTAP–DOPC > DOTAP–DC-Chol–DOPC–DOPE > DC-Chol–DOPE–DMPC.

Fig. 7 shows the SAXS patterns of DC-Chol–DOPE/DNA lipoplexes in the time interval from 10 min to 48 h after the addition of negatively charged MM liposomes at $R=0.4$ compared to that of DC-Chol–DOPE/DNA lipoplexes with no anionic lipid added ($R=0$). The swelling of the lamellar phase is clearly shown by the shift of the (*002*) Bragg peak as indicated by the vertical dashed line. Shortly after the addition of the negatively charged liposomes, a considerable decrease in DNA packing density (i.e. increase in d_{DNA}) was detected with d_{DNA} changing from 38.1 Å ($R=0$) to 47.0 Å ($R=0.4$; $t=10$ min). In the top panel of Fig. 7 the change in inter-DNA distance with time is shown. After 1 h only minor changes in DNA packing density (less than 1 Å) were detected.

Similar experiments were also carried out on other lipoplexes (not illustrated) and gave analogous results. We did not find any sensible correlation between lipoplexes formulation and equilibration time of lipoplexes/anionic liposomes mixed systems. Our kinetic results are in good agreement with those reported by the MacDonald's group. These authors reported on the kinetics of phase changes in lipoplexes upon addition of anionic lipids using SAXS [11,41]. In very recent papers, they showed that structural changes [11] and DNA release [41] reaches a plateau after about 1 h.

3.5. Effect of DNA size and morphology on the structure of lipoplexes

In principle, it is questionable to compare lipoplexes containing short fragments of linear DNA (used in SAXS experiments) with those where larger plasmid DNA were employed (electrophoresis and TE measurements). To explore the effect of size and morphology of DNA (linear or plasmid) on the structure of lipoplexes, we performed SAXS experiments on both CL/linear DNA/DOPG and CL/plasmid DNA/DOPG mixed systems. Fig. 8 shows the comparison between the structure of DOTAP–DOPC/linear DNA/DOPG and DOTAP–DOPC/plasmid DNA/DOPG lipoplexes. The DNA packing is, within experimental errors, the same: $d_{DNA}=42.6$ and 43.1 Å for linear DNA-containing and plasmid DNA containing-lipoplexes, respectively. Minor changes could be observed in the shape and width of the DNA peak thereby reflecting a more pronounced structural disorder, when plasmid DNA was used. However, the final structure of lipoplexes did not severely depend on the DNA used. When interacting with DOPG, structural changes of lipoplexes containing linear or plasmid DNA were essentially the same. At $R=1$ (Fig. 8), SAXS patterns of DOTAP–DOPC/linear DNA/DOPG and DOTAP–DOPC/plasmid DNA/DOPG lipoplexes were practically superimposable.

3.6. DNA release from lipoplexes induced by anionic lipids

The extent of DNA release from different lipoplex formulations after interaction with anionic liposomes was investigated by electrophoresis on agarose gels as a function of increasing *R*. The gel electrophoresis assay allows to determine how much DNA is completely free from lipid, while other techniques, such as the fluorescence resonance energy transfer assay, may overestimate DNA release, since it includes also DNA that is no longer electrostatically associated with cationic lipids, but still entrapped within the lipid aggregate [42]. The intensity of free DNA bands (not illustrated), varied significantly with lipid formulations.

Fig. 9 shows that X_{DNA} increases with increasing *R*. At each *R* value, the molar fraction of released DNA was in the following order: DOTAP–DOPC > DOTAP–DC-Chol–DOPC–DOPE > DC-Chol–DOPE–DMPC. The latter observation correlates well with our SAXS experiments. Indeed, our results indicated that the fraction of DNA released from lipoplexes by anionic lipids varies significantly with lipid formulations: the most stable lipoplexes display the lowest extent of DNA release, while lipoplexes with the highest propensity to be disintegrated by anionic lipids (DOTAP–DOPC/DNA) also exhibit much larger DNA release. Lipoplexes with intermediate resistance to disintegration also exhibited intermediate values of X_{DNA}. We therefore emphasize that electrophoresis experiments confirmed the existence of a strict correlation between destabilization of lipoplexes and DNA unbinding.

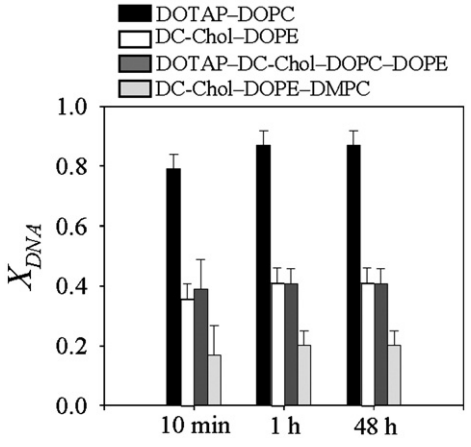

Fig. 10. Molar fraction of released DNA, X_{DNA}, as a function of time for the anionic/cationic charge ratio $R=5$. Within 1 h after addition of the negatively charged lipoplexes, the molar fraction of released DNA, X_{DNA}, reached its plateau value.

Table 2
Hydrodynamic radius, R_H, of lipoplexes as a function of increasing number of lipid components, n: DOTAP–DOPC/DNA (A), DC-Chol–DOPE/DNA (B), DOTAP–DC-Chol–DOPC–DOPE/DNA (C), DOTAP–DC-Chol–DOPC–DOPE–DMPC–DLPC/DNA (2:2:1:1:1:1) (D)

Lipoplexes	n	R_H (nm)
A	2	214±50
B	2	180±39
C	4	205±47
D	6	195±45

Where not specified, lipid species were in an equimolar ratio.

3.7. Kinetics of DNA release from lipoplexes induced by anionic lipids

Given the kinetic structural changes of lipoplexes, it was desirable to measure, as a function of time, the release of DNA from lipoplexes induced by addition of DOPG liposomes. Thus, we performed electrophoresis experiments to investigate the temporal evolution of the molar fraction of DNA, X_{DNA}, that dissociated from the lipid surface and was liberated from the lipoplexes [42]. Measurements were initiated immediately after addition of the anionic liposomes and replicated after 10 min, 1 h and 48 h. The results are presented in Fig. 10 for the unique anionic/cationic charge ratio $R=5$, however, the kinetics of DNA release was found not to depend severely on R (not reported). As evident, the lipoplex formulations tested did not show any appreciable difference in the kinetics of DNA release. Within 1 h after addition of the negatively charged lipoplexes, X_{DNA}, reached its plateau value. These results were in very good agreement with the kinetic structural changes of lipoplexes illustrated in Fig. 7 and with previously reported data [41].

3.8. Size of lipoplexes

Transfection efficiency is known to be affected by the size of complexes. Thus, we performed DLS experiments to investigate the effect of size on the lipoplex efficiency. Given that the transfection pattern (Fig. 1) increases monotonically with the number of lipid components, n, it was attractive to investigate the effect of n on the size of lipoplexes and, in turn, on their efficiency. Thus, we examined the hydrodynamic radius of the tested lipoplexes (Table 2). We did not find any significant correlation neither between size and n nor between size and transfection efficiency. Thus, the size of the tested multicomponent lipoplexes is not a major determinant of lipofection efficiency.

4. Discussion

Elucidating the mechanism of lipid-mediated gene delivery is of central importance to improve the transfection efficiency of lipoplexes. A number of physical–chemical properties of lipoplexes have been proposed as factors regulating transfection efficiency. In the present study, we investigated some physical–chemical characteristics that might account for the superior transfection efficiency of the most efficient lipoplexes such as their lipid composition, structure, propensity to be disintegrated by anionic lipids and ability to release DNA.

In Fig. 1 we showed that multicomponent lipoplexes, incorporating from three to six lipid species simultaneously, presented much higher TE (about two orders of magnitude) than binary lipoplexes usually employed for gene delivery. Furthermore, a trend was found that the transfection activity increases with the number of lipid components, n, with some exceptions due to lipid composition. In principle, this finding may be related to the higher fusogenicity [18] and compatibility [19] of vesicles made of several lipid components with respect to single lipids. Indeed, even though the significance of lipid diversity in biological membranes still remains obscure, it is expected to play a role in formation of non-bilayer phases, membrane interaction and fusion and biocompatibility [17–20].

Recently, the Safinya's group identified membrane charge density of cationic vesicles, σ_M, as a universal parameter that governs transfection efficiency of lamellar complexes *in vitro* [34]. In particular, the existence of an optimal membrane charge density was demonstrated and efficiency data were found to merge onto a universal, bell-shaped curve as a function of σ_M. In the present investigation, we prepared cationic liposomes with significant variations in membrane composition but only slight differences in membrane charge density (Table 1). Indeed, all lipoplex formulations we tested ($0.0076<\sigma_M<0.0098$ e/Å^2) lie in a narrow region, where transfection efficiency is roughly constant as a function of σ_M [34]. In contrast, we found remarkable differences in transfection efficiency due to lipid composition (Fig. 1). Furthermore, the discovery that a high transfection efficiency can be achieved by employing multicomponent complexes at a lower-than-ever-before membrane charge density of lipoplexes was of primary significance. On the basis of the most accredited evidences reported in the literature so far [34], we advance the concept that not only membrane charge density, but also other factors, such as lipid composition, may be important in regulating TE of lipoplexes.

In search of the reason why multicomponent lipoplexes were definitely more efficient than binary ones, we investigated the structural changes of lipoplexes upon interaction with anionic lipids. It is well established that the structure of lipoplexes can be modified by interaction with anionic lipids, and that phase behaviour of lipoplexes may control their TE [9–13]. SAXS results suggest the existence of three different scenarios. In the first range ($0<R<1$) the DNA load was continuously decreased by the addition of anionic lipids as shown by the shift of the DNA peak (Fig. 4). But, in the same range of R, electrophoresis measurements indicated that DNA was very poorly released (Fig. 9). The enlargement in DNA–DNA distance (Fig. 4, top panel) can be essentially attributed to the augmentation of anionic lipids within the lipoplex [16]. In the second range, starting from $R\sim1$, disintegration of the initial multilamellar structure of lipoplexes took place. As above introduced, we defined R^* as the anionic/cationic charge ratio at which lipid bilayer disintegration was completed. For $1<R<R^*$ the SAXS patterns of each lipoplex/DOPG mixture were characterized by simultaneous vanishing of diffraction peaks arising from the lamellar phase of lipoplexes and appearance of Bragg reflections

of the lamellar phase of pure DOPG. Third, further increase in anionic lipid ($R > R^*$) leads to a one-phase range, where the system was identified with the L_α phase of pure DOPG (Fig. 3). While all the lipoplexes tested exhibited the same general phase behaviour, relevant differences in their propensity to be destroyed by anionic lipids were detected. Indeed, each lipoplex formulation exhibited a specific value at which the lamellar structure of lipoplexes was completely disintegrated, i.e. a specific R^* value.

In principle, the correlation between structural stability of lipoplexes and transfection activity may be attributed to the fact that interaction of lipoplexes with anionic membranes resulted in facilitated or impeded DNA release. In this context, lipoplex formulations exhibiting different affinity for anionic lipids may therefore account for structural changes of lipoplexes and, in turn, for varying transfection efficiency. To correlate structural changes of lipoplexes with TE behaviour, the first step was to verify that disintegration of lamellar lipoplexes really resulted in DNA release. We therefore measured the extent of DNA release from lipoplexes induced by anionic lipids. To this end, we chose three mixtures (DOTAP–DOPC/DNA, the less resistant mixture to be disintegrated; DC-Chol–DOPE–DOPC/DNA, the most resistant mixture to be disintegrated; DOTAP–DC-Chol–DOPC–DOPE/DNA, one mixture exhibiting an intermediated behaviour). Fig. 9 shows that the extent of DNA release estimated by electrophoresis was in excellent agreement with structural stability of lipoplexes revealed by synchrotron SAXS. The most unstable lipoplexes (DOTAP–DOPC/DNA) rapidly released DNA, while the most stable complexes (DC-Chol–DOPE–DOPC/DNA) exhibited a lower extent of DNA release. Thus, we provided experimental evidence that the higher the structural stability, the lower the extent of DNA release. For instance, in the case of DOTAP–DOPC/DNA lipoplexes (Fig. 9, black bars) completion of DNA release (as revealed by electrophoresis), a crucial requirement for transfection, occurred close to $R \sim 5$. This value is in good agreement with R^* as determined by SAXS. We therefore emphasize that our combined results proved the existence of the supposed correlation between destabilization of lipoplexes and DNA unbinding.

Accurate knowledge of R^* for each lipoplex formulations may help towards rational design of lipoplexes and controlled DNA release. Anyway, our findings are not in good agreement with previously reported data [42]. Indeed, it has been recently proposed that increased instability and diminished retention of DNA can account for enhanced transfection activity by lipoplexes. Even though structural stability and DNA release are undoubtedly correlated, as we have clearly shown, the same cannot be claimed for TE and DNA release. For instance, DOTAP–DC-Chol–DOPC–DOPE/DNA lipoplexes were much more efficient (about two orders of magnitude) than DOTAP–DOPC/DNA lipoplexes (Fig. 1), while the latter complexes exhibited a much higher propensity to be destroyed by anionic lipids and to release DNA (Fig. 9). The case of DOTAP–DOPC/DNA lipoplexes is highly paradigmatic. These complexes were the most unstable ones when interacting with negatively charged liposomes, exhibited the lowest R^* compared to all the lipoplex formulations tested and showed the highest propensity to release DNA (Fig. 9). According to the statement of Wang et al. [38], one would expect that DOTAP–DOPC/DNA lipoplexes were also the most efficient ones. On the opposite, their marked structural instability and poor retention of DNA did not result in high transfection efficiency (Fig. 1).

One question spontaneously arises: How can we explain the discrepancy between our findings and those reported by Wang et al.? A closer look reveals that experiments performed by us and by Wang et al. [42] are to some extent different. Indeed, we investigated the structural changes of lipoplexes as a function of R in order to find the specific anionic/cationic charge ratio, R^*, needed to disintegrate the lamellar phase of lipoplexes completely and release all delivered DNA. Conversely, Wang et al. [42] performed experiments at a specific R value ($R \sim 0.2$). Such a value was presumably chosen because it models the interaction between lipoplexes and the plasma membrane.

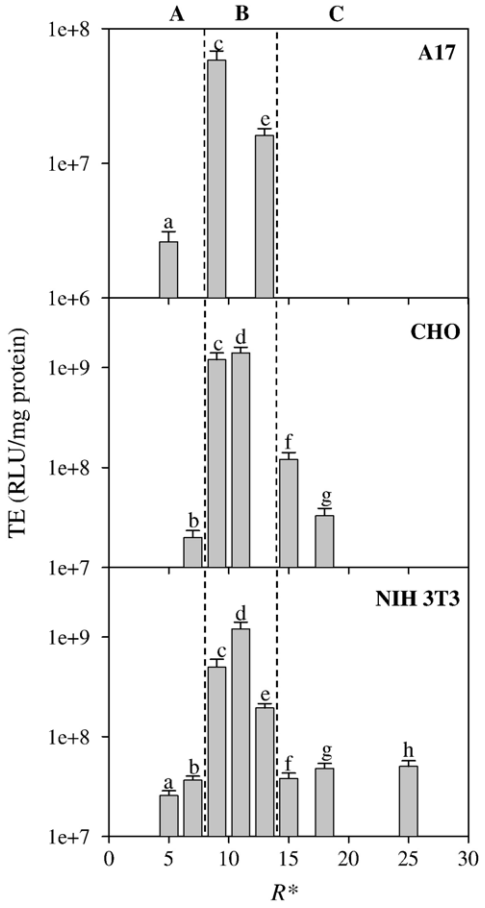

Fig. 11. TE in RLU/mg of cellular proteins plotted as a function of R^* referring to disintegration of lipoplexes by DOPG for the cell lines: NIH 3T3 (bottom panel), CHO (middle panel) and A17 (top panel). DOTAP–DOPC/DNA (a); DC-Chol–DMPC/DNA (b); DOTAP–DC-Chol–DOPC–DOPE/DNA (c); DOTAP–DC-Chol–DOPC–DOPE–DLPC–DMPC/DNA (d); DC-Chol–DOPE/DNA (e); DOTAP–DOPC–DLPC/DNA (f); DOTAP–DLPC/DNA (g); DC-Chol–DOPE–DMPC/DNA (h). Vertical dashed lines identified three regimes of stability: low (A), medium (B) and high (C). In the top panels, regimes of stability could not be accurately clarified (vertical dashed lines were located according to the bottom panel).

Interaction between lipoplexes and anionic membranes may be central in lipid-mediated transfection. Thus, some considerations should be made. When a lipoplex with membrane charge density σ_M comes into contact with an anionic membrane with membrane charge density σ_A, the anionic/cationic charge ratio at the contact surface is roughly given by $R'=\sigma_A/\sigma_M$. Moreover, at the molecular level, at least two cases of DNA release may be considered: (i) the release from lipoplexes is a single event; (ii) the DNA release is gradual involving multiple interactions with the cellular membranes.

Considering the tested lipoplex formulations, a rough estimation gives $R' \sim 2$ and 0.7 for DOPG and MM liposomes, respectively. We observed that the anionic/cationic charge molar ratio at which lipoplex disintegration was completed, R^*, was much higher than R'. Thus, our findings clearly suggest that multiple interactions are absolutely necessary to release DNA significantly. It is currently believed, that in cells lipoplexes may interact with a number of cellular membranes during which DNA may be gradually released. Hence, we emphasize that investigating the dependence of DNA release on R (Fig. 9) is a critical point that needs to be deeply investigated. On the contrary, the correlation between ease of DNA release and transfection efficiency was observed by Wang et al. [42], when the interaction between lipoplexes and anionic membranes is likely to be a one step process (i.e. at low R). However, at low R ($R<0.5$), all the lipoplex formulations tested by us and by Wang et al. [42] released only a minor part of their gene freight (Fig. 9). At present, it is not clear if lipid-mediated transfection involves single or multiple interactions with anionic membranes. If interaction between lipoplexes and anionic membranes would be a single event, as one can model by performing measurements at a single R value, the scenario proposed by Wang et al. [42] is persuasive. In this case, poor DNA release is the limiting transfection factor. Conversely, if multiple step release occurs, TE and ability in DNA release are not proportional to each other.

A deeper insight to the TE data suggests a more complex scenario. When plotted against R^*, it becomes obvious that the TE data coalesce into a single quasi-Gaussian curve (Fig. 11). Fig. 11 suggests the existence, of three regimes. In the first regime (regime A), one finds complexes that were easily solubilized by anionic lipids. Such complexes (labelled as a and b) were inefficient (TE$<10^8$ RLU/mg protein). In regime B, lipoplexes exhibit the highest efficiency (TE$>10^8$ RLU/mg protein). In regime C, corresponding to highly stable complexes that resisted disintegration by anionic lipids (high R^* values), again low efficiency is given. Regime B appears therefore to be as the 'region of optimal stability'. Even though the bell-shaped curve of TE vs. R^* is better expressed in the case of NIH 3T3 cell line (Fig. 11, bottom panel), similar trends are also observed with ovarian CHO and tumoral A17 cell lines (Fig. 11, middle and top panel, respectively). The universality of the observed behavior was confirmed by the diversity of the employed cell lines [43,44]. Although the mechanism of interaction of lipoplexes with cell membranes has not been clarified so far, recent works have confirmed the general expectation that endocytosis is the principal machinery of entry of lamellar lipoplexes [45,46]. After cellular uptake via endocytosis, lipoplexes must escape from endosomes in order for the DNA to move toward the cell nucleus. As Fig. 11 clearly shows, poorly efficient lipoplexes are either unstable against disintegration by anionic lipids (Fig. 11, regime A) or resist them (Fig. 11, regime C).

Another point to address is the influence, of charge density of the anionic membranes. Given that interaction between lipoplexes and anionic liposomes involves some local contact, charge densities of lipoplexes and anionic liposomes must affect the membrane interaction. Therefore, we investigated the interaction between lipoplexes and MM liposomes. Indeed, in MM liposomes the anionic charge carried by DOPG molecules is diluted by neutral lipids and the resulting membrane charge density is definitely lower than that of pure DOPG liposomes. SAXS results of Fig. 6 indicate that, disintegration of lipoplexes by MM liposomes occurs at higher R^* values than those needed when using pure DOPG liposomes. Hence, the lower the membrane charge density of anionic liposomes employed, the higher the amount of anionic lipid needed to destroy lipoplexes. As a consequence, the bell-shaped "TE versus R^* distribution of Fig. 11 shifts to higher values (Fig. 12). This indicates that membrane charge density of anionic liposomes severely affects

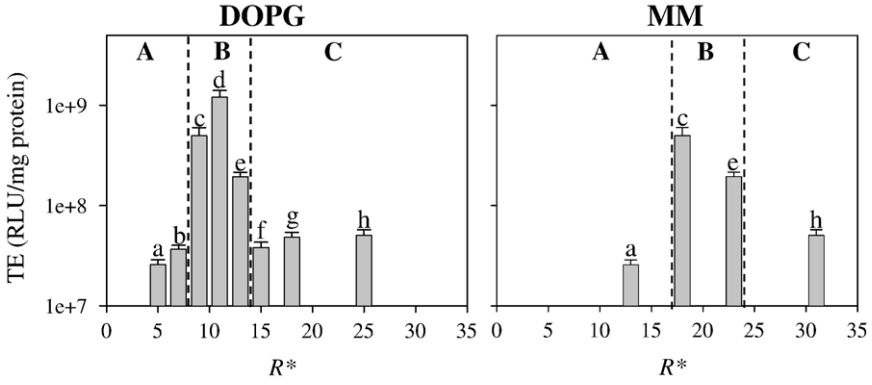

Fig. 12. TE in RLU/mg of cellular proteins plotted as a function of R^* referring to disintegration of lipoplexes by DOPG (left panel) and by MM liposomes (right panel) for the mouse fibroblast cell line (NIH 3T3). DOTAP–DOPC/DNA (a); DC-Chol–DMPC/DNA (b); DOTAP–DC-Chol–DOPC–DOPE/DNA (c); DOTAP–DC-Chol–DOPC–DOPE–DLPC–DMPC/DNA (d); DC-Chol–DOPE/DNA (e); DOTAP–DOPC–DLPC/DNA (f); DOTAP–DLPC/DNA (g); DC-Chol–DOPE–DMPC/DNA (h).

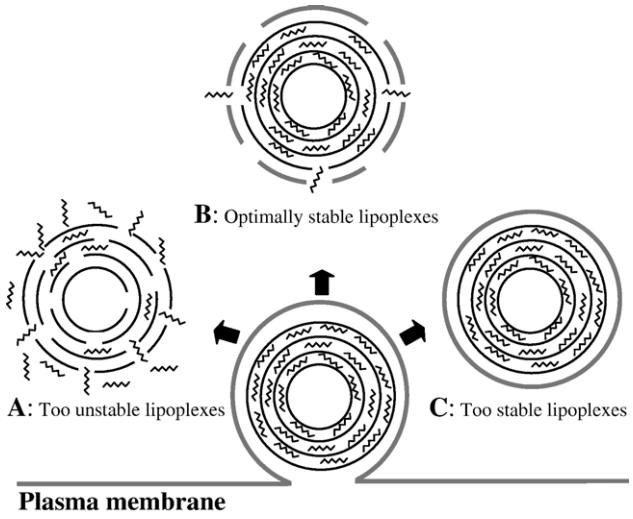

Fig. 13. Schematic cartoon showing the proposed mechanism of the cellular uptake of lipoplexes and DNA release. Unstable lipoplexes rapidly fuse with anionic lipids and release DNA in the cytoplasm (A). Too stable lipoplexes (C) retain their lamellar organization after interaction with negatively charged membranes and poorly release DNA. 'Optimally stable' lipoplexes (B) release their major freight only after having reached the cell nucleus.

the structural stability of lipoplexes. However, the general conclusions drawn from the liposomes interactions remain valid.

The representation illustrated in Fig. 13 summarizes our present hypothesis of the molecular events occurring at the early stages of internalization of lipoplexes within the cell. Electrostatic attractions let the lipoplex approach the anionic surface of the cell and attachment is followed by endocytosis resulting in endosomal entrapment. Our SAXS and electrophoresis experiments seem to suggest that the less stable lipoplexes dissociate early in the cytoplasm and easily release DNA. As a result unstable lipoplexes are less efficient (Fig. 11, regime A), because lipoplex might dissociate in the cytoplasm instead of the nuclei. If too fast dissociation is a critical attribute of poor transfection, the same might be claimed for poor DNA release resulting in entrapment within endosomal structures (Fig. 11, regime C) [12,13,35]. 'Optimally stable' lipoplexes (Fig. 11, regime B) may release delivered DNA gradually in the cytoplasm, the event occurring through interactions with anionic molecules, which readily form complexes with cationic vesicles.

5. Conclusion

We have investigated the structure-efficiency relationship of lamellar lipoplexes. Further, we have shown that multicomponent lipoplexes are superior in transfection with respect to binary lipoplexes which are usually employed in worldwide gene delivery trials. Efficiency of lipoplexes was found to increase with the number of lipid components the carrier is composed of. The lipid composition may also influence lipoplex lipid exchange with cellular membranes and release of DNA. Such multicomponent combinations of lipids synergistically enhance transfection efficiency and appear very appropriate for analyzing the origin of the diverse activity of lipoplex formulations with difference in chemical composition.

It is commonly thought that, lipoplexes enter the cell by endocytosis [45,46] and that a direct correlation between transfection efficiency and extent of DNA release does exist. We have made some efforts to clarify transfection route by relating structural evolution of lipoplexes upon interaction with anionic lipids and extent of DNA release. We have provided evidence that destabilization and fusion of lamellar lipoplexes results in continuous DNA release. We have also shown that the structural disintegration of lipoplexes caused by anionic lipids helps to judge their TE. Since both unstable and too stable lipoplexes result in strong and poor DNA release respectively, and exhibit low transfection efficiency, we have established structural stability upon interaction with anionic molecules as a key parameter governing the transfection efficiency of lipoplexes. The discovered regime of 'optimal stability' (Fig. 11, regime B) seems therefore to be a reasonable compromise between too rapid DNA release and endosomal entrapment of lipoplexes in the cytoplasm. Careful adjusting of lipoplex composition to generate the 'proper interaction' between lipoplexes and anionic lipids should therefore help to optimize synthetic lipid-based transfection agents. The adoption of rationally designed lipoplexes would ensure that users definitely improve transfection efficiency of lipid carriers.

Acknowledgments

We sincerely thank the Reviewers for the many useful suggestions offered to improve this article. Prof. C. Cametti is acknowledged for allowing us to use the Malvern Zetasizer4 apparatus located at the Department of Physics of the University of Rome 'La Sapienza'. Prof. C. Cametti is also gratefully acknowledged for extensive and interesting discussions.

References

[1] P.L. Felgner, G.M. Ringold, Cationic liposome-mediated transfection, Nature 337 (1989) 387–388.
[2] T. Salditt, I. Koltover, J.O. Rädler, C.R. Safinya, Self-assembled DNA-cationic lipid complexes: two-dimensional smectic ordering, correlations and interactions, Phys. Rev. E 58 (1998) 889–904.
[3] I. Koltover, T. Salditt, J.O. Rädler, C.R. Safinya, An inverted hexagonal phase of cationic liposome–DNA complexes related to DNA release and delivery, Science 281 (1998) 78–81.
[4] T. Salditt, I. Koltover, J.O. Rädler, C.R. Safinya, Two-dimensional smectic ordering of linear DNA chains in self-assembled DNA-cationic liposome mixtures, Phys. Rev. Lett. 79 (1997) 2582–2585.
[5] G. Caracciolo, D. Pozzi, R. Caminiti, A. Congiu Castellano, Structural characterization of a new lipid/DNA complex showing a selective transfection efficiency in ovarian cancer cells, Eur. Phys. J. E 10 (2003) 331–336.
[6] A.J. Lin, N.L. Slack, A. Ahmad, C.X. George, C.E. Samuel, C.R. Safinya, Three-dimensional imaging of lipid gene-carriers: membrane charge density controls universal transfection behavior in lamellar cationic liposome–DNA complexes, Biophys. J. 84 (2003) 3307–3316.
[7] G. Caracciolo, R. Caminiti, Do DC-Chol/DOPE-DNA complexes really form an inverted hexagonal phase? Chem. Phys. Lett. 411 (2005) 327–332.
[8] A. Congiu, D. Pozzi, C. Esposito, G. Mossa, Correlation between structure and transfection efficiency: a study of DC-Chol–DOPE/DNA complexes, Colloids Surf., B Biointerfaces 36 (2004) 43–48.
[9] R. Koynova, L. Wang, R.C. MacDonald, An intracellular lamellar–nonlamellar phase transition rationalizes the superior performance of some

cationic lipid transfection agents, Proc. Natl. Acad. Sci. U. S. A. 103 (2006) 14373–14378.
[10] Y.S. Tarahovsky, R. Koynova, R.C. MacDonald, DNA release from lipoplexes by anionic lipids: correlation with lipid mesomorphism, interfacial curvature, and membrane fusion, Biophys. J. 87 (2004) 1054–1064.
[11] R. Koynova, L. Wang, Y. Tarahovsky, R.C. MacDonald, Lipid phase control of DNA delivery, Bioconjug. Chem. 16 (2005) 1335–1339.
[12] L. Wasungu, M.C. Stuart, M. Scarzello, J.B. Engberts, D. Hoekstra, Lipoplexes formed from sugar-based gemini surfactants undergo a lamellar-to-micellar phase transition at acidic pH. Evidence for a non-inverted membrane-destabilizing hexagonal phase of lipoplexes, Biochim. Biophys. Acta 1758 (2006) 1677–1684.
[13] D. Hoekstra, J. Rejman, L. Wasungu, F. Shi, I. Zuhorn, Gene delivery by cationic lipids: in and out of an endosome, Biochem. Soc. Trans. 35 (2007) 68–71.
[14] G. Caracciolo, D. Pozzi, H. Amenitsch, R. Caminiti, Multicomponent cationic lipid–DNA complex formation: role of lipid mixing, Langmuir 21 (2005) 11582–11587.
[15] G. Caracciolo, D. Pozzi, R. Caminiti, H. Amenitsch, Lipid mixing upon deoxyribonucleic acid-induced liposomes fusion investigated by synchrotron small-angle x-ray scattering, Appl. Phys. Lett. 87 (2005) 133901–133903.
[16] G. Caracciolo, D. Pozzi, R. Caminiti, C. Marchini, M. Montani, A. Amici, H. Amenitsch, DNA release from cationic liposome/DNA complexes by anionic lipids, Appl. Phys. Lett. 89 (2006) 2339031–2339033.
[17] J. Heyes, L. Palmer, K. Bremner, I. MacLachlan, Cationic lipid saturation influences intracellular delivery of encapsulated nucleic acids, J. Control. Release 107 (2005) 276–287.
[18] W. Lin, C.D. Blanchette, M.L. Longo, Fluid-phase chain unsaturation controlling domain microstructure and phase in ternary lipid bilayers containing GalCer and cholesterol, Biophys. J. 92 (2007) 2831–2841.
[19] M.A. Alonso, J. Millán, The role of lipid rafts in signalling and membrane trafficking in T lymphocytes, J. Cell Sci. 114 (2001) 3957–3965.
[20] S. Pautot, B.J. Frisken, D.A. Weitz, Engineering asymmetric vesicles, Proc. Natl. Acad. Sci. 100 (2003) 10718–10721.
[21] G. Caracciolo, R. Caminiti, D. Pozzi, M. Friello, F. Boffi, A. Congiu Castellano, Self-assembly of cationic liposomes–DNA complexes: a structural and thermodynamic study by EDXD, Chem. Phys. Lett. 351 (2002) 222–228.
[22] D. Pozzi, H. Amenitsch, R. Caminiti, G. Caracciolo, How lipid hydration and temperature affect the structure of DC-Chol-DOPE/DNA lipoplexes, Chem. Phys. Lett. 422 (2006) 439–445.
[23] H. Amenitsch, M. Rappolt, M. Kriechbaum, H. Mio, P. Laggner, S. Bernstorff, First performance assessment of the small-angle X-ray scattering beamline at ELETTRA, J. Synchrotron Radiat. 5 (1998) 506–508.
[24] V. Luzzati, P. Mariani, H. Delacroix, X-ray crystallography at macromolecular resolution: a solution of the phase problem, Makromol. Chem., Macromol. Symp. 15 (1988) 1–17.
[25] O. Francescangeli, D. Rinaldi, M. Laus, G. Galli, B. Gallot, An X-ray study of a smectic C and smectic A liquid crystal polyacrylate, J. Phys., II 6 (1996) 77–89 (France).
[26] R. Zantl, L. Baicu, F. Artzner, I. Sprenger, G. Rapp, J.O. Rädler, Thermotropic phase behavior of cationic lipid–DNA complexes compared to binary lipid mixtures, J. Phys. Chem., B 103 (1999) 10300–10310.
[27] G. Caracciolo, D. Pozzi, H. Amenitsch, R. Caminiti, One-dimensional thermotropic dilatation area of lipid headgroups within lamellar lipid/DNA complexes, Langmuir 22 (2006) 4267–4273.
[28] F. Bordi, C. Cametti, S. Sennato, Polyions act as an electrostatic glue for mesoscopic particle aggregates, Chem. Phys. Lett. 409 (2005) 134–138.
[29] M.C. Pedroso de Lima, S. Simões, P. Pires, H. Faneca, N. Duzgunesü, From biophysics to biological applications, Adv. Drug Deliv. Rev. 47 (2001) 277–294.
[30] I.S. Zuhorn, D. Hoekstra, On the mechanism of cationic amphiphile-mediated transfection. To fuse or not to fuse: is that the question? J. Membr. Biol. 189 (2002) 167–179.
[31] F. Artzner, R. Zantl, G. Rapp, J.O. Rädler, Observation of a rectangular columnar phase in condensed lamellar cationic lipid–DNA complexes, Phys. Rev. Lett. 81 (1998) 5015–5018.
[32] A.S Narang, L. Thoma, D.D. Miller, R.I. Mahato, Cationic lipids with increased DNA binding affinity for nonviral gene transfer in dividing and nondividing cells, Bioconjug. Chem. 16 (2005) 156–168.
[33] K.K Ewert, A. Ahmad, H.M. Evans, C.R. Safinya, Cationic lipid–DNA complexes for non-viral gene therapy: relating supramolecular structures to cellular pathways, Expert Opin. Biol. Ther. 5 (2005) 33–53.
[34] A. Ahmad, H.M. Evans, K. Ewert, C.X. George, C.E. Samuel, C.R. Safinya, New multivalent cationic lipids reveal bell curve for transfection efficiency versus membrane charge density: lipid–DNA complexes for gene delivery, J. Genet. Med. 7 (2005) 739–748.
[35] I.S Zuhorn, U. Bakowsky, E. Polushkin, W.H. Visser, M.C.A. Stuart, J.B.F.N. Engberts, D. Hoekstra, Nonbilayer phase of lipoplex–membrane mixture determines endosomal escape of genetic cargo and transfection efficiency, Mol. Ther. 11 (2005) 801–810.
[36] I. Koltover, T. Salditt, C.R. Safinya, Phase diagram, stability, and overcharging of lamellar cationic lipid–DNA self-assembled complexes, Biophys. J. 77 (1999) 915–924.
[37] I. Koltover, K. Wagner, C.R. Safinya, DNA condensation in two-dimensions, Proc. Natl. Acad. Sci. U. S. A. 97 (2000) 14046–14052.
[38] G. Caracciolo, R. Caminiti, DNA–DNA electrostatic interactions within cationic lipid/DNA lamellar complexes, Chem. Phys. Lett. 400 (2004) 314–319.
[39] G. Caracciolo, D. Pozzi, R. Caminiti, H. Amenitsch, Two-dimensional lipid mixing entropy regulates the formation of multicomponent lipoplexes, J. Phys. Chem., B 110 (2006) 20829–20835.
[40] B. Pozo-Navas, V.A. Raghunathan, J. Katsaras, M. Rappolt, K. Lohner, G. Pabst, Discontinuous unbinding of lipid multibilayers, Phys. Rev. Lett. 91 (2003) 028101–028104.
[41] R. Koynova, Y. Tarahovsky, L. Wang, R.C. MacDonald, Lipoplex formulation of superior efficacy exhibits high surface activity and fusogenicity, and readily releases DNA, Biochim. Biophys. Acta 1768 (2007) 375–386.
[42] L. Wang, R. Koynova, H. Parikh, R.C. MacDonald, Transfection activity of binary mixtures of cationic O-substituted phosphatidylcholine derivatives: the hydrophobic core strongly modulates their physical properties and DNA delivery efficacy, Biophys. J. 91 (2006) 3692–3706.
[43] M. Galiè, M. D'Onofrio, M. Montani, A. Amici, L. Calderan, P. Marzola, D. Benati, F. Merigo, C. Marchini, A. Sbarbati, Tumor vessel compression hinders perfusion of ultrasonographic contrast agents, Neoplasia 7 (2005) 528–536.
[44] M. Galiè, C. Sorrentino, M. Montani, L. Micossi, E. Di Carlo, T. D'Antuono, L. Calderan, P. Marzola, D. Benati, F. Merigo, F. Orlando, A. Smorlesi, C. Marchini, A. Amici, A. Sbarbati, Mammary carcinoma provides highly tumourigenic and invasive reactive stromal cells, Carcinogenesis 26 (2005) 1868–1878.
[45] S. Mukherjee, R.N. Ghosh, F.R. Maxfield, Endocytosis, Physiol. Rev. 77 (1997) 759–803.
[46] P. Chabaud, M. Camplo, D. Payet, G. Serin, L. Moreau, P. Barthelemy, M.W. Grinstaff, Cationic nucleoside lipids for gene delivery, Bioconjug. Chem. 17 (2006) 466–472.